Chapter 13

QSARs and Three-Dimensional Shape Studies of Fungicidal Azolylmethylcyclopentanols

Molecular Design of Novel Fungicides Metconazole and Ipconazole

Hiroshi Chuman[1], Atsushi Ito[2], Toshihide Saishoji[2], and Satoru Kumazawa[2]

[1]Intelligent Systems Development for Research Department, Kureha Chemical Industry Company, Ltd., 3–25–1 Hyakunin-cho, Shinjuku-ku, Tokyo 169, Japan
[2]Nishiki Research Laboratory, Kureha Chemical Industry Company, Ltd., 16 Ochiai, Nishiki-machi, Iwaki-shi, Fukushima 974, Japan

A series of azole compounds containing a cyclopentane ring were synthesized and tested for fungicidal activity. The Hansch-Fujita type QSAR and three-dimensional shape comparison analyses were employed to optimize the structure of a lead compound logically for the higher fungicidal activity, resulting in the discovery of metconazole and ipconazole, promising fungicides of novel structure. A possible mode of interaction between metconazole and its target receptor, cytochrome $P450_{14DM}$ was proposed.

Since the end of 1960s, a number of so-called azole type fungicides, which show their antifungal activity by inhibiting the C-14 demethylation step of the ergosterol biosynthetic pathway, have been investigated in both academia and industry over the world (*1*). Hundreds of patents covering azole type fungicides have been published and over twenty new compounds have been introduced commercially for agricultural use. As seen in the structures of a number of azole type fungicides, the most general structure requirements for the activity is considered to contain a nitrogen-containing heteroaromatic (azole) ring, a hydroxy group and a benzene ring. According to the number of chemical bonds intervening between the azole and the benzene rings, fenarimol (**I**) and fluotrimazole (**II**) are classified in the two-bond type, and most of other typical fungicides such as triadimefon (**III**), propiconazole (**IV**), cyproconazole (**V**), diniconazole (**VI**), flusilazole (**VII**) and triflumizole (**VIII**) are classified in the three-bond type, as shown in Figure 1.

We have synthesized a series of azolylmethylcyclopentanols, classified as the five-bond type and measured their antifungal activities against plant pathogens *in vitro* and *in vivo*. Among them, we have discovered metconazole (**IX**) and ipconazole (**X**) also shown in Figure 1, which show a high fungicidal activity and a broad spectrum against various plant diseases. The safety studies have confirmed their low-toxicity for mammals, birds, and aquatic organisms and also have proved their degradability in the environment. Metconazole (**IX**) was launched in the spring of 1994 in France for

0097–6156/95/0606–0171$12.00/0

controlling important cereal pests such as septoria and fusarium diseases, and rusts and leaf blotches. At the same time, ipconazole (**X**) was introduced for controlling seedborne rice diseases in Japan.

This paper focuses on the lead optimization processes, during which the traditional Hansch-Fujita type analyses of the quantitative structure-activity relationships (QSAR) and three-dimensional shape comparisons gave essential contributions to achieving the discovery.

Two-bond type :

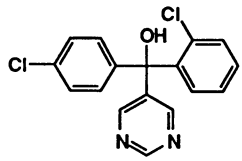

fenarimol (**I**)

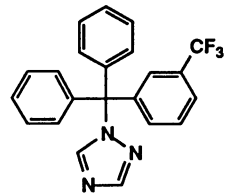

fluotrimazole (**II**)

Three-bond type :

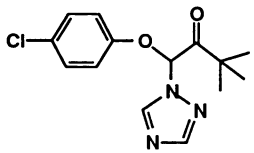

triadimefon (**III**)

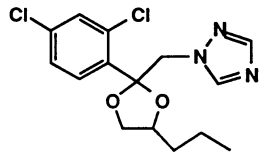

propiconazole (**IV**)

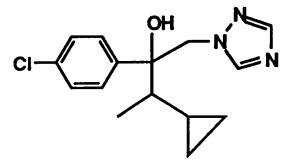

cyproconazole (**V**)

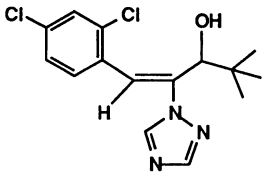

diniconazole (**VI**)

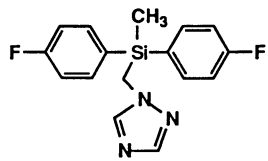

flusilazole (**VII**)

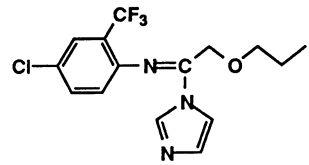

triflumizole (**VIII**)

Five-bond type :

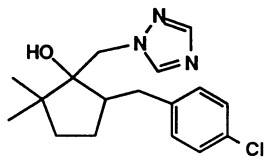

metconazole (**IX**)

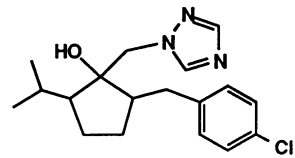

ipconazole (**X**)

Figure 1. Typical and novel azole type fungicides for agricultural use.

Materials and Methods

Compounds : The synthesis of compounds **1–34** is briefly outlined in Figure 2 (for details, see Jpn. Kokai Tokkyo Koho JP62-149667, 1987; JP1-93574, 1989). The compounds were classified into types I and II according to those without and with the R_1, R_2-substituents, respectively, and listed in Tables I and II separately. Each diastereo-isomeric set containing enantiomers (racemate) was isolated at the step of the epoxide intermediate. The configuration of the triazolyl compounds shown in Figure 2 is that of the active form. Compounds **1–32** were used for the QSAR studies. Compounds **19**, **33** and **34** were optically resolved by the normal phase high-performance liquid chromatography (HPLC) with a chiral column (CHIRALCELL OD 500 mm x 10 mm i.d., DAICEL Chemical Industries Ltd.). The chemical purity (p), specific rotation and enatiometric excess (ee) were as follows : (–)-**19** ; p = 100.0 %, $[\alpha]_{20}^{D}$ = –23.7° (c = 10.0, EtOH), ee = 100.0 %, (–)-**33** ; p = 99.9 %, $[\alpha]_{20}^{D}$ = –3.3° (c= 1.23, EtOH), ee = 99.8 %, (–)-compound **34** ; p = 98.2 %, $[\alpha]_{20}^{D}$ = –24.4° (c = 1.11, EtOH), ee = 96.4 %. (±)-compounds **19** and **33** are, respectively, metconazole and ipconazole.

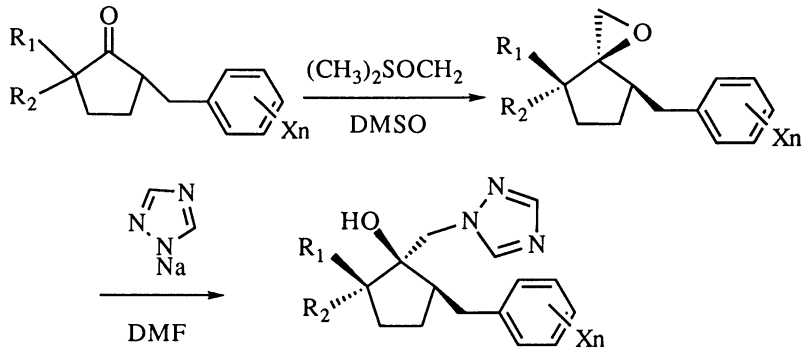

Figure 2. Synthetic scheme. For absolute configuration, see below.

Antifungal Activities *in vitro* : Each test compound was dissolved and diluted with dimethyl sulfoxide (DMSO), and then suspended in sterilized potato sucrose agar (PSA) medium to give prescribed concentrations (the final DMSO concentration was 1 %). The medium was poured in petri dishes and was hardened. Mycelial discs (4 mm in diameter) of *Botrytis cinerea* and *Gibberella fujikuroi* grown on the PSA alone in advance were transferred to the PSA plates containing the various concentrations of each compound and incubated. The diameter of each colony was measured to determine the IC_{50} value (the effective concentration in M for 50 % inhibition of mycelial growth). The pIC_{50} (*in vitro*) is listed in Tables I and II. For some compounds, the minimum inhibitory concentration (MIC) in μg/ml against various fungal species was recorded. The incubation was performed at 20 or 28°C for 2 or 3 days, depending on fungal species.

Antifungal Activities *in vivo* : The each type I compound was dissolved in acetone and suspended in water (the final acetone concentration was 5 %) with 60 μg/ml of a detergent, Gramin S. The suspension was diluted with water containing 5% of acetone and 60μg/ml of Gramin S to give a series of prescribed concentrations and was sprayed on a cucumber seedling at the first leaf stage. After 4 hours of the chemical treatment, two mycelial discs (4 mm in diameter) of *Botrytis cinerea* grown on the PSA

In Classical and Three-Dimensional QSAR in Agrochemistry; Hansch, Corwin, et al.;
ACS Symposium Series; American Chemical Society: Washington, DC, 1995.

Table I. Antifungal Activities and Physicochemical and Steric Parameters of Triazolylmethylcyclopentanols (Type I)

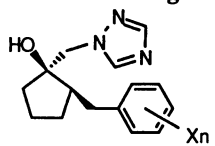

Compounds [a]		Log P [b]	Steric Parameters of PhXn (Å) [c]				pIC$_{50}$ [d] (*in vitro*)						(*in vivo*)	
							B.c. [e]			*G.f.* [f]			*B.c.* [e]	
No.	Xn		L1	L2	W	D	obsd.	calcd.[g]	calcd.[h]	obsd.	calcd.[i]	calcd.[j]	obsd.	calcd.[k]
1	H	2.26*	3.68	2.48	6.70	3.48	4.6	5.01	4.97	4.8	5.12	5.08	2.9	3.24
2	2-Cl	2.95	3.68	3.30	7.79	3.50	3.8	3.83	4.12	4.3	4.37	4.83	1.9	2.41
3	3-Cl	2.98	3.68	2.48	7.79	3.50	4.7	4.93	4.77	5.0	5.08	4.85	1.9	2.41
4	3-CF_3	3.07	4.11	2.48	8.29	4.83	3.9	3.62	3.51	4.2	4.21	4.13	1.9	1.83
5	4-Cl	3.11*	4.86	2.48	6.70	3.50	6.1	5.95	5.80	5.9	5.95	5.77	3.8	3.55
6	4-F	2.39	4.22	2.48	6.70	3.48	5.1	5.21	5.14	5.3	5.28	5.23	3.3	3.38
7	4-Br	3.27*	5.10	2.48	6.70	3.70	5.9	5.89	5.75	5.9	5.96	5.77	4.1	3.45
8	4-CF_3	3.07	4.85	2.48	6.70	4.83	5.3	4.97	4.88	—[l]			3.2	3.57
9	4-CH_3	2.71*	4.68	2.48	6.70	3.97	5.4	5.26	5.16	5.5	5.42	5.40	3.5	3.58
10	4-*t*-Bu	3.97*	5.75	2.48	6.71	6.16	3.9	4.20	4.25	5.1	5.11	5.06	1.9	2.37
11	4-Ph	3.92*	7.96	2.48	6.70	3.48	6.2	6.13	6.05	—[l]			2.2	2.49
12	4-CN	1.70	5.56	2.48	6.70	3.48	4.2	3.96	4.09	4.3	4.29	4.25	2.5	2.24
13	2,4-Cl_2	3.87	4.86	3.30	7.79	3.50	4.4	4.13	4.47	4.9	4.80	4.96	1.9	1.40
14	2,4-F_2	2.60	4.22	2.84	7.20	3.48	4.7	4.59	4.67	5.0	4.86	5.04	3.2	2.99
15	2-F,4-Cl	3.27	4.86	2.84	7.20	3.50	5.2	5.14	5.18	5.5	5.39	5.43	3.3	2.90
16	2,6-F_2	2.60	3.68	2.84	7.70	3.48	3.7	4.17	4.24	4.3	4.51	4.65	2.1	2.45
17	3,4-F_2	2.51	4.22	2.48	7.20	3.48	5.3	4.95	4.85	5.6	5.07	4.96	3.3	2.93
18	2,3,4,5,6-F_5	3.16	4.22	2.84	7.70	3.48	4.5	4.67	4.70	4.8	4.98	5.01	2.7	2.43

For footnotes, see Table II.

Table II. Antifungal Activities and Physicochemical and Steric Parameters of Triazolylmethylcyclopentanols (Type II)

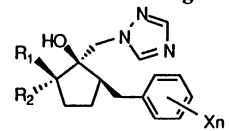

Compounds [a]				Log P [b]	Steric Parameters of PhXn (Å) [c]				pIC50 [d] (*in vitro*)			
					L1	L2	W	D	*B.c.* [e]		*G.f.* [f]	
No.	R1	R2	Xn						obsd.	calcd.[h]	obsd.	calcd.[j]
19	Me	Me	4-Cl	3.83*	4.86	2.48	6.70	3.50	6.6	6.47	6.8	6.84
20	Me	Me	4-F	3.11	4.22	2.48	6.70	3.48	6.4	6.24	6.6	6.79
21	Me	Me	4-Br	3.99	5.10	2.48	6.70	3.70	6.5	6.33	6.9	6.74
22	Me	Me	4-CH_3	3.43	4.68	2.48	6.70	3.97	6.5	6.07	6.8	6.75
23	Me	Me	4-*t*-Bu	4.69	5.75	2.48	6.71	6.16	3.8	4.40	5.5	5.55
24	Me	Me	4-Ph	4.64	7.96	2.48	6.70	3.48	6.1	6.23	6.1	6.33
25	Me	Me	2-F,4-Cl	3.99	4.86	2.84	7.20	3.50	6.2	5.75	6.7	6.39
26	Me	Me	3-OH,4-Cl	3.16	4.86	2.48	7.27	3.50	5.1	5.76	6.7	6.35
27	Et	H	4-Cl	4.02*	4.86	2.48	6.70	3.50	6.4	6.46	6.7	6.78
28	Et	H	4-F	3.30	4.22	2.48	6.70	3.48	6.0	6.34	6.6	6.85
29	Et	H	4-Br	4.18	5.10	2.48	6.70	3.70	6.4	6.29	6.7	6.64
30	Et	H	2,4-Cl_2	4.78	4.86	3.30	7.79	3.50	5.1	4.55	5.5	5.31
31	Et	H	4-*t*-Bu	4.88	5.75	2.48	6.71	6.16	4.6	4.25	5.3	5.33
32	Et	H	4-Ph	4.83	7.96	2.48	6.70	3.48	5.9	6.51	6.2	6.12
33	*iso*-Pr	H	4-Cl	4.28*					6.4		6.9	
34	H	Et	4-Cl	3.71*					— [l]		— [l]	

a) Tested as the racemate of enatiomers the configuration of which is shown above. b) Asterisked values were measured.
c) Definitions of steric parameters are described in the text. d) $pIC_{50} = -\text{Log } IC_{50}$ (M)
e) *B.c.* : *Botrytis cinerea* f) *G.f.* : *Gibberella fujikuroi* g) Calculated by equation 4. h) Calculated by equation 7.
i) Calculated by equation 5. j) Calculated by equation 8. k) Calculated by equation 6. l) — : not measured.

In Classical and Three-Dimensional QSAR in Agrochemistry; Hansch, Corwin, et al.;
ACS Symposium Series; American Chemical Society: Washington, DC, 1995.

medium alone in advance were inoculated on the first foliage leaf of the cucumber treated with each concentration of the test compounds. The plants were kept in 100 % humidity at 20°C for 3 days. The IC_{50} value (the effective concentration in M in the sprayed suspension for 50 % inhibition of the disease expansion) was determined from the diameter of each infected area. The pIC_{50} (*in vivo*) is listed in Table I.

Partition Coefficient (Log P) : Partition coefficients (P) of type I compounds, **1, 5, 7, 9, 10** and **11,** were measured in the octanol-water system by the shaking-flask method. By using the reversed phase HPLC, k' value for the same set of compounds was also measured . k' is defined as the ratio of retention times : $(t - t_0) / t_0$, where t_0 is the retention time of a reference compound, fructose, and t is that of each test compound. A good linear relationship between log P and log k' was obtained for these compounds as shown in equation 1.

$$\log P = 3.77 \log k' + 2.93 \quad (1)$$
$$n = 6,\ r = 0.975,\ s = 0.166$$

In this and the following equations 4 – 8, n is the number of data used in the correlation, r is the multiple correlation coefficient and s is the standard deviation. Each term in equations 1 and 4 – 8 was confirmed as being significant above the 95 % level. Log P values of the other type I compounds was calculated from the k' value and equation 1. Log P value of type II compounds, **19, 27, 33** and **34,** were measured by the shaking-flask method. Log P value of the other type II compounds was estimated by the additive rule: *i.e.*, by adding π values of alkyl substituents calculated from measured log P values of compounds **5, 19** and **27** to the log P of the compounds without alkyl substituents. Tables I and II list log P value of compounds used in this study. The log P value of typical azole fungicides, **III, IV, VI, VII** and **VIII,** were newly measured as shown below.

Steric Parameters : In order to describe steric influences of substituents in the phenyl moiety, we introduced steric parameters similar to the STERIMOL (*2*) in our QSAR equations. Definitions of steric parameters are shown in Figure 3. L_1 and L_2 denote the maximum length of *para*- and *ortho*-substituents from the center of the benzene ring along the x-axis direction, respectively. W and D are the measure of the maximum width of the substituted benzene ring in two directions perpendicular to the x-axis. The relevant steric parameters are listed in Tables I and II.

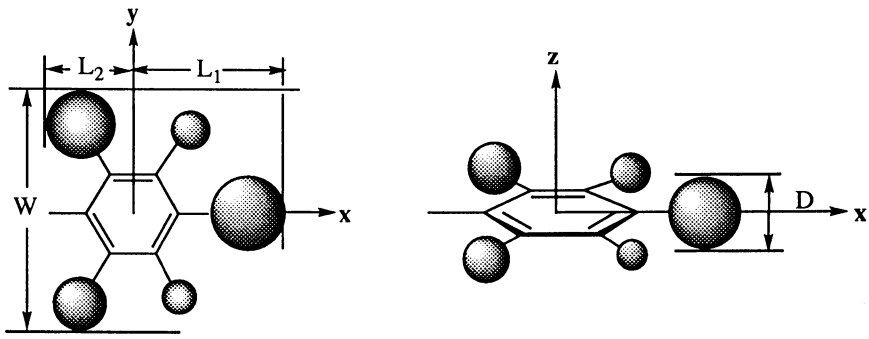

Figure 3. Definition of the steric parameters.

Superposition and Conformation Analyses : The least-squares superposing in terms of corresponding atomic positions is the most widely used method. This method superposes two molecules, A and B, by minimizing a target function F* indicated as equation 2.

$$F^* = \Sigma \omega_i \mid r_{Ai} - r_{Bi} \mid^2 \quad (2)$$

r_{Ai} (r_{Bi}) : i th corresponding atomic position vector of the molecule A (B).
ω_i : weight of i th corresponding pair.

It should be noted, however, that this method is generally limited to rigid molecular systems. The function value of F* is sensitive to small variations in conformation. It is generally difficult to find the best superposition because the value of F* depends on a given conformation of the molecule A (B). The compounds treated here contain rotatable bonds around which conformational changes affect the value of F*. In order to consider this conformational flexibility, we introduced torsion angle variables that express conformational freedom of molecules and we also added a term arising from the conformational energy change, $\Delta E(\Theta_A)$ ($\Delta E(\Theta_B)$) of the molecule A (B) (Chuman, H., unpublished work).

$$F = \Sigma \omega_i \mid r_{Ai}(\Theta_A) - r_{Bi}(\Theta_B) \mid^2 + S [\Delta E(\Theta_A) + \Delta E(\Theta_B)] \quad (3)$$

$r_{Ai}(\Theta_A)$ [$r_{Bi}(\Theta_B)$] : i th corresponding atomic position vector, r_{Ai} (r_{Bi}), is a function of torsion angles, Θ_A (Θ_B) for the molecule A (B).
S : scaling factor in the dimension of square distance / energy.

For minimizing the target function F, the first term only with fixed torsion angles was first minimized by the Monte Carlo method which overcomes local minimum problems (*4*) and then the minimization of the total F value as the function of the torsion angles was performed. The second term in equation 3 was estimated by a force field similar to ECEPP (*3*) in which independent variables are torsion angles only.

In computational conformation analysis, we generated initial conformers by a combination of the grid search (*4*) (systematically changing the angular increment of each rotatable bond) and the ring conformation search (*5*) (a systematic conformation search with ring closure constraints), and then optimized these structures with MNDO (*6*). In the superposition of molecules mentioned above, each optimized structure obtained by MNDO was used as the starting conformation in which torsion angles were initial values of the independent variable set, Θ, in the target function F.

Results and Discussion

QSAR(I) : Series of type I compounds (**1**–**18**) with various substituents in the phenyl moiety were assayed for the antifungal activity against *Botrytis cinerea in vitro* as well as *in vivo* and against *Gibberella fujikuroi in vitro*. The results seem to show that the optimal substituents on the phenyl moiety are *para*-chloro and bromo. The corresponding compounds (**5** and **7**) are among the most active *in vitro* as well as *in vivo* as seen from Table I. To validate this, variations in the antifungal activity were examined using physicochemical and steric parameters and regression analyses. Electronic parameters of Xn substituents such as the Hammett σ were not statistically significant. Equations 4–6 gave the best correlation quality among various combinations of log P, the steric parameters, L_1, L_2, W and D, and squared terms of these parameters. Negative signs of parameter terms in equations 4–6 suggest that the phenyl moiety is accommodated inside a sterically restricted hydrophobic pocket of the target receptor site. The difference in the optimum log P value for the activity against *Botrytis cinerea* between *in vitro* and *in vivo* (3.71 and 2.87, respectively) seems to reflect a

difference in the transport process to the target site under respective conditions. While the favorable substitution patterns in some other azole type fungicides are 2,4-dihalo (*7*) as found in propiconazole (**IV**), diniconazole (**VI**) and triflumizole (**VIII**), the QSAR results show the substituent on the 2 (*ortho*) position of the benzene ring is definitely unfavorable for the activity because of the negative coefficients of the L_2 term in equations 4 and 5. The introduction of bulkier substituents to the *para* position is also unfavorable because of the negative W and D terms. Only introduction of a moderately hydrophobic substituent into the *para* position seems to enhance the activity because of its dependence on the log P. With these QSAR considerations, we confirmed and selected the *para*-chloro derivative (compound **5**) as the most promising lead compound for the next step.

$$\text{pIC}_{50}\ (\textit{Botrytis cinerea in vitro}) = -1.309\ L_2 - 0.843\ W - 0.716\ D + 4.023 \log P - 0.541 (\log P)^2 + 10.068 \quad (4)$$
$$n = 18,\ r = 0.952,\ s = 0.282,\ \log P^{opt} = 3.71$$

$$\text{pIC}_{50}\ (\textit{Gibberella fujikuroi in vitro}) = -0.833\ L_2 - 0.711\ W - 0.435\ D + 2.896 \log P - 0.356 (\log P)^2 + 8.735 \quad (5)$$
$$n = 16,\ r = 0.938,\ s = 0.237,\ \log P^{opt} = 4.07$$

$$\text{pIC}_{50}\ (\textit{Botrytis cinerea in vivo}) = -1.090\ W + 5.781 \log P - 1.008 (\log P)^2 + 2.624 \quad (6)$$
$$n = 18,\ r = 0.854,\ s = 0.425,\ \log P^{opt} = 2.87$$

The log P value of the lead compound **5**, 3.11, is approximately 0.8 smaller than the averaged value (3.88) of typical fungicides **III** (log P = 3.11), **IV** (3.54), **VI** (4.30), **VII** (3.97) and **VIII** (4.50) in Figure 1, and the calculated molecular volume of compound **5**, 262 Å^3, is also slightly smaller than the averaged volume (*ca.* 280 Å^3) of the same set of compounds. Considering these physicochemical structural features, we moved to the next logical step for the further enhancement of the activity.

Three-Dimensional (3D) Shape Comparison : Compound **5** has two asymmetric carbons and hence two racemic geometrical isomers. The relative configuration of the isomer responsible for the antifungal activity was examined by ^{1}H NMR-NOE experiments which measure NOE signals between benzyl and triazol-1-ylmethylene protons in two geometrical isomers. No intensity increase according to the NOE effect was observed in the more active isomer, whereas there was a considerable increase in the less active one. The relative configuration of the active isomer of compound **5** was thus concluded to be (1*S*,2*S*) or (1*R*,2*R*) (the *cis* arrangement of the hydroxy and benzyl groups as shown in Figure 2 and Table I).

We planned to increase the hydrophobicity and molecular volume of compound **5** for higher antifungal activity. A number of such analogs are conceivable. However, the results of the QSAR(I) indicate no more space for introducing hydrophobic substituents into the phenyl moiety. Therefore, as a possible choice, we tried to introduce *gem*-dimethyl at the 5 position of the cyclopentane ring of compound **5** leading to compound **19** (metconazole) (note changes in the stereochemical notation and the atom numbering of compounds **5** and **19**, see Figure 4).

In spite of the broad diversity in the 2D structure of azole type fungicides, their 3D structures are assumed to take similar shapes which are complementary to the binding site in the target receptor. From this assumption, we carried out the 3D shape comparison calculation between compound **19** and diniconazole (**VI**) as the reference

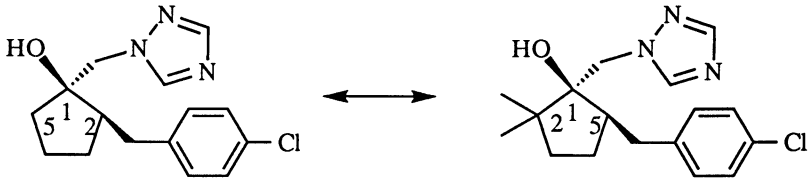

(1*R*,2*R*)-compound **5** (1*S*,5*R*)-compound **19**

Figure 4. The stereochemical and the atom numbering relation between compounds **5** and **19** (metconazole).

simultaneously with the synthetic effort of compound **19**. Diniconazole is reported(*8,9*) to show a high antifungal activitiy (pIC_{50} (M) *in vitro* for *Botrytis cinerea* = 5.5 and for *Gibberella fujikuroi* = 5.9 under slightly different experimental conditions). Each energy minimum conformer of compound **19** obtained by MNDO was compared to that of diniconazole by the superposition method described above. The active configuration of diniconazole was reported as (*R*) (common name : diniconazole M) as shown in the right hand side of Figure 5. Katagi (*10*) reported the existence of two major conformers, I and II, which are different in the torsion angle around the C-C bond to which *tert*-butyl and hydroxy groups are attached geminally. Without a large change in the conformational energy (the second term in equation 3) from that of the starting conformer (local energy minimum conformer obtained by MNDO), the (1*S*,5*R*) configuration of compound **19** was superposable on the conformer II of (*R*)-diniconazole with the smallest root mean square value and the second largest common volume among the four possible pairs as shown in Table III. Figure 5 shows the *gem*-dimethyl of compound **19** and *tert*-butyl group of diniconazole appear to occupy almost the same geometric region. Thus, we considered that the alkyl groups at the 2 position on the cyclopentane ring of compound **19** play an important role for the antifungal activity. Simultaneously, the active configuration of compound **19** was assumed as (1*S*,5*R*) and its active conformation is shown in Figure 5.

Table III. Three-dimensional Shape Comparison between Isomers of Compound 19 (Metconazole) and Those of Diniconazole [a]

Compound **19** [b]	Diniconazole [b]	RMSD [c] (Å)	Common volume (Å^3)
(1*S*,5*R*)	(*R*) conformer I	1.13	203
(1*S*,5*R*)	(*R*) conformer II	0.57	211
(1*R*,5*S*)	(*R*) conformer I	0.75	220
(1*R*,5*S*)	(*R*) conformer II	0.87	196

a) 8 pairs of corresponding atoms circled in structural formulae in Figure 5 were used in this comparison.
b) As those in which the value of F in equation 3 is minimum.
c) Root Mean Square Deviation values.

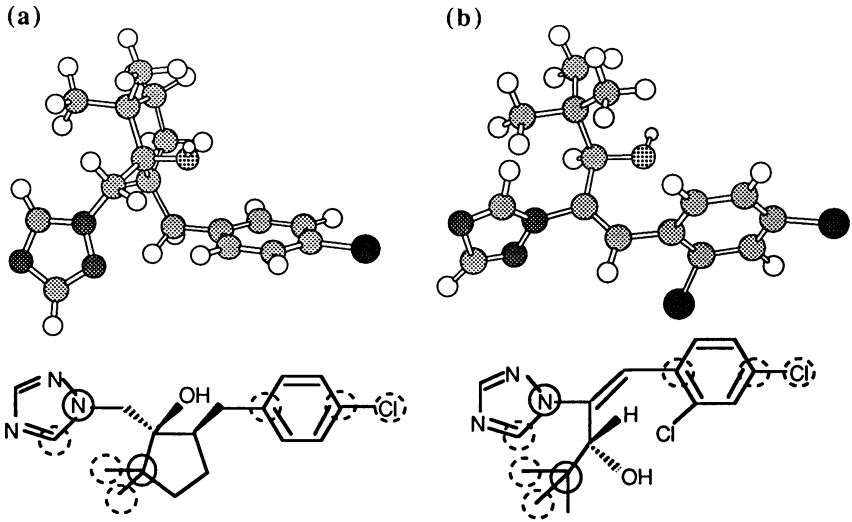

Figure 5. Three-dimensional shape comparison of the (1*S*,5*R*)-isomer of compound **19** (metconazole) (a) and the conformer II of (*R*)-diniconazole (b). Atoms enclosed by circles are used in the three-dimensional superposition and the value ω_i in equation 3 is assigned as two for the atoms in solid and unity for ones in broken circles, respectively.

The optical isomers of compound **19** were prepared and their *in vitro* antifungal activity was measured against a number of phytopathogenic fungi. Table IV lists the MIC values in comparison with that of the lead compound **5**. The (–) isomer of compound **19** indeed showed an excellent activity with a broad fungitoxic spectrum.

Table IV. MIC Values (μg/ml) of Compounds 5 and 19 (Metconazole)

Compounds	Pathogenic Fungi								
	P.o.	*G.f.*	*F.c.*	*B.c.*	*S.s.*	*S.c.*	*G.c.*	*C.b.*	*A.m.*
(±)–**5**	25	6.25	>100	6.25	6.25	0.78	25	12.5	100
(±)–**19**	6.25	0.39	1.56	1.56	1.56	<0.2	1.56	25	25
(–)–**19**	3.13	<0.2	0.78	0.39	0.78	<0.2	0.78	25	12.5
(+)–**19**	100	50	>100	25	>100	1.56	50	>100	>100

P.o. : *Pyricularia oryzae*
F.c. : *Fusarium oxysporum f. sp.cucumerinum*
S.s. : *Sclerotinia sclerotiorum*
G.c. : *Glomerella cingulata*
A.m. : *Alternaria mali*
G.f. : *Gibberella fujikuroi*
B.c. : *Botrytis cinerea*
S.c. : *Sclerotinia cinerea*
C.b. : *Cercospora beticola*

In other words, the introduction of alkyl groups at the 5- position on the cyclopentane ring of the lead compound **5** caused a remarkable increase of the antifungal activity . Our prediction based upon the QSAR and the 3D shape comparison studies was thus confirmed. As another choice to increase the hydrophobicity and substructual molecular volume of compound **5** in its 5-position substituents, we synthesized compound **33** (the isopropyl derivatives, ipconazole) and confirmed its high fungicidal activity. The absolute configuration and active conformation of the antifungally active compounds **19** and **33**, remains to be verified.

X-Ray Crystallographic and Conformational Analyses : In order to assign directly the absolute configuration of antifungally active isomers of the type II compounds, we carried out a single crystal X-ray analysis of the antifungally more active enantiomers of compounds **19**, **33** and **34** (the Et derivative), all of which resolved isomers were optically minus. Their crystal structures were determined as follows : (–)-compound **19** ; monoclinic, $P2_1$, a = 9.015, b = 12.581, c = 7.321 Å, γ = 96.84°, Z = 2, R = 0.0576 , (–)-compound **33** ; monoclinic, $P2_1$, a = 23.592, b = 8.448, c = 9.973 Å, β = 113.54°, Z = 4, R = 0.0450, and (–)-compound **34** ; orthorhombic, $P2_12_12_1$, a = 18.132, b = 10.455, c = 8.745 Å, Z = 4, R = 0.0628.

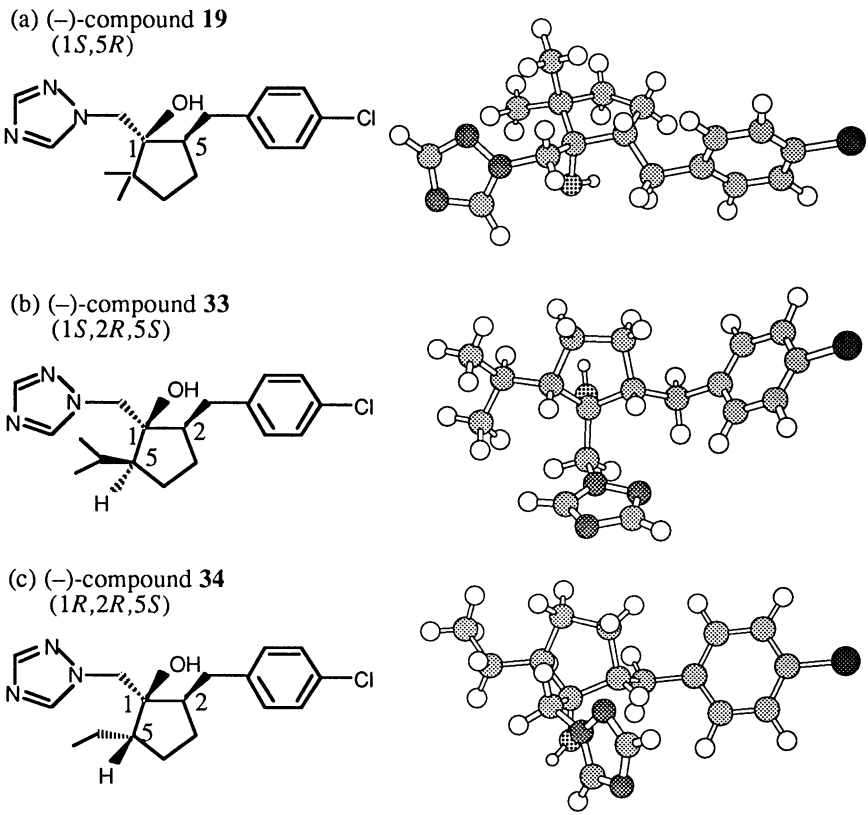

Figure 6. The absolute configuration and the crystal structure of the antifungal (–)-isomers of compounds **19** (metconazole) (a), **33** (ipconazole) (b) and **34** (c).

All the above packing structures contain an intermolecular hydrogen bond between the hydroxyl group and the nitrogen atom at the 4 position of the triazole ring. The X-ray structure analysis assigned the absolute configurations of the above (–)-compounds **19**, **33** and **34** as (1*S*,5*R*), (1*S*,2*R*,5*S*) and (1*R*,2*R*,5*S*), respectively, as shown in Figure 6. These assignments are to verify the above assumption from the 3D shape comparison study. The configuration of four ligands around each of the 1- and 2-carbon atoms in type I compounds and each of the 1-, 2-, and 5-carbon atoms in compounds **19–32** is reasonably considered to be the same as that around the corresponding carbon atoms in the above compounds as far as the most active diastereomer is concerned. Therefore, the absolute configuration of compounds as presumed in Figure 2 and Tables I and II seems to be valid.

In compounds listed in Tables I and II, torsion angles, θ_1 and θ_2, of which definitions are shown in Figure 7(a), determine the spatial placement of the two important aromatic rings, triazole and benzene. The values, (θ_1,θ_2) in the crystal structures are (181°, 176°), (52°, 186°) and (–51°, 161°) for (–)-compounds **19**, **33** and **34**, respectively. These angles possibly indicate the general conformational feature of all the compounds discussed in this paper. The conformation with respect to θ_1 for the triazol-1-ylmethyl is considered to be flexible, whereas that with respect to θ_2 for the benzyl is considered to be fixed in the *trans* vicinity to the triazole ring. To investigate the conformation profile and to examine the relevancy of the active conformation predicted by the 3D shape comparison study as shown in Figure 5, we carried out an extensive conformational search of (–)-(1*S*,5*R*)-compound **19** using a semiempirical molecular orbital method, MNDO. We found that there are three major local enery minimum conformers. For these conformers, (θ_1,θ_2) were (191°, 196°), (53°, 187°) and (–66°, 185°). These three sets of (θ_1,θ_2) are close to the observed ones of (–)-compounds **19**, **33** and **34** in the crystal structures, respectively. Energies of these three conformers exist in a small range of values, being 0.8 (181°, 176°), 3.9 (52°, 186°) and 5.4 (–51°, 161°) kcal/mol higher than that of the ground energy minimum, (191°, 196°), respectively. The active conformation predicted in Figure 5(a) takes a folded structure, where (θ_1,θ_2) is located at a region, (*ca.* 60°, *ca.* 60°). This conformation gives a rather high energy value, *ca.*10 kcal/mol from the ground minimum energy. This energy value locates just on the border line for the criterion to select the active conformation as the reasonable one, when errors inherent in MNDO and the neglect of other possible factors affecting the stability such as an energy gain from the binding with the target receptor are taken into account (*11*). In order to clarify this point, we synthesized a conformationally fixed analog, compound **35**, shown in Figure 7(b). Compound **35** takes only the *trans* conformation around the double bond,

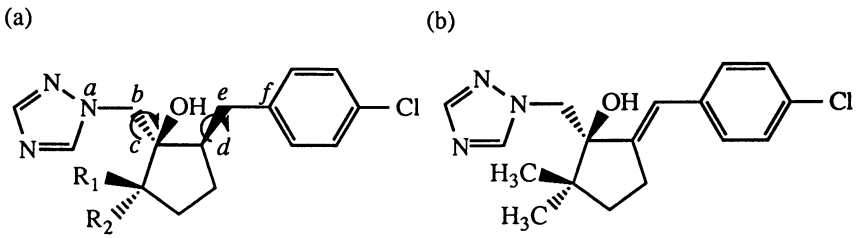

Figure 7. (a) Definition of torsion angles and (b) structure of compound **35**. The torsion angles, θ_1 and θ_2, are defined by the sequential atoms, a-b-c-d and c-d-e-f, respectively.

i.e., θ_2 = *ca.* 180°. Its antifungal activity was much lower (MIC value for *Gibberella fujikuroi* = 6.25 μg/ml) than that of compound **19** (0.39 μg/ml). In general, it is difficult to determine the active conformation explicitly unless a direct X-ray crystallographic analysis of an inhibitor-receptor complex could be performed. However, we tentatively could conclude that the active conformation takes (*ca.* 60°, *ca.* 60°) as the set of torsion angle values, (θ_1,θ_2).

QSAR(II) : The activity potentiating effect of the alkyl substituents on the cyclopentane ring was quantitatively examined to formulate equations 7 and 8, by introducing an indicator variable *I* into equations 4 and 5. The indicator variable, *I* takes zero and unity for type I and type II compounds, respectively. The sign and size of the respective terms, except for the indicator variable in equations 7 and 8, are almost equivalent to those of the corresponding terms in equations 4 and 5. The indicator variable term is statistically significant and the sign is positive. From a point of view independently from the 3D shape comparison results, equations 7 and 8 also support that the alkyl groups on the cyclopentane ring play an important role in binding with the target receptor.

$$\begin{aligned} &pIC_{50} \text{ (*Botrytis cinerea in vitro*, type I + type II)} \\ &= -0.761\ L_2 - 0.862\ W - 0.669\ D + 3.237 \log P - 0.418 (\log P)^2 + 0.428\ I \\ &\quad +9.782 \qquad (7) \\ &\quad n = 32,\ r = 0.933,\ s = 0.377,\ \log P^{opt} = 3.87 \end{aligned}$$

$$\begin{aligned} &pIC_{50} \text{ (*Gibberella fujikuroi in vitro*, type I + type II)} \\ &= -0.790\ W - 0.270\ D + 3.350 \log P - 0.471 (\log P)^2 + 1.012\ I + 6.145 \qquad (8) \\ &\quad n = 30,\ r = 0.966,\ s = 0.245,\ \log P^{opt} = 3.56 \end{aligned}$$

The binding mode of metconazole and ipconazole to the cytochrome $P450_{14DM}$: Based upon the results obtained, the proposed binding mode of (–)-compound **19**, *i.e.*, (1*S*,5*R*)-metconazole to the target receptor, cytochrome P450 catalyzing lanosterol 14α-demethylation ($P450_{14DM}$) (*12*) is illustrated in Figure 8. The following interactions at the molecular level are proposed :

1. The nitrogen atom at the 4 position of the triazole ring coordinates to the heme ferric ion in $P450_{14DM}$.
2. The presence of the hydroxy group at the 1 position of the cyclopentane ring was experimentally confirmed to be indispensable for the activity (unpublished data). This group is considered to be involved in either hydrogen bonding or electrostatic interaction with an amino acid residue in the close proximity of the active site of $P450_{14DM}$.
3. The QSAR(I) results suggest the existence of a hydrophobic pocket or groove, which accommodates the *para*-chloro-phenyl group, in the proximity of the active site.
4. The 3D shape comparison, the QSAR(II) results and the enhancement of the activity with the introduction of *gem*-dimethyl (metconazole) and isopropyl groups (ipconazole) to the cyclopentane ring indicate that the *gem*-dimethyl and isopropyl groupings play an essential role in binding with $P450_{14DM}$. These structures are possibly assigned as another hydrophobic interaction site.

Poulos *et al* . (*13*) reported the crystal structure of the cytochrome P450 camphor 5-exohydroxylase ($P450_{cam}$) as the camphor bound form. It is difficult to obtain direct information as to the binding mode of metconazole from their results because of a low homology of amino acid sequences between $P450_{14DM}$ and $P450_{cam}$ (*14*). However, the binding site of metconazole in $P450_{14DM}$ is supposed to be surrounded by hydrophobic amino acid residues, similar to the camphor binding site in $P450_{cam}$.

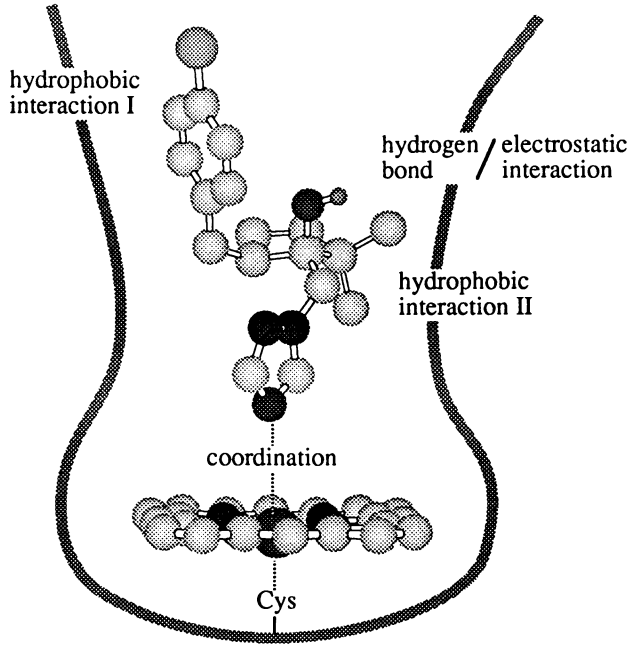

Figure 8. Schematic diagram illustrating the binding of (1*S*,5*R*)-metconazole to cytochrome $P450_{14DM}$.

Concluding Remarks

We have been successful in developing the novel potent fungicides of great promise, metconazole (**19**) and ipconazole (**33**). In this paper, we focused on the processes of structural modification from a lead compound to metconazole and ipconazole. During these processes, QSAR analyses of the Hansch-Fujita type and three-dimensional shape comparisons of molecules played critical roles. Furthermore, these procedures have made a great contribution to a deeper understanding of the binding mode of azole type fungicides to the target receptor, $P450_{14DM}$.

Finally, we would like to stress that the discovery of metconazole and ipconazole are from a careful and synergistic cooperation of our synthetic, biological and physical-chemical scientists over a period of several years.

Acknowledgments

We are indebted to Dr. Chizuko Kabuto of Tohoku University for the X-ray measurements. We would like to express our sincere thanks to our many colleagues involved in this special project in Kureha Chemical Industry Co., Ltd., in particular, Drs. Masaaki Takahashi and Yasuo Amagi who have organized this project and led us.

Literature Cited

1. Köller, W. *Pestic. Sci.* **1987**, *18*, 129.
2. Verloop, A.; Hoogenstraaten, W.; Tipker, J. In *Drug Desin Vol. VII* ; Ariëns, E. J. Ed.; Academic Press: New York, **1976**; pp. 165-206.

3. Momany, F. A.; McGuire, R. F.; Burgess, A. W.; Scheraga, H. A. *J. Phys. Chem.* **1975**, *79*, 2361.
4. Leach, A. R. In *Reviews in Computational Chemistry , Volume 2* ; Lipkowitz, K. B.; Boyd, D. B., Ed.; VCH Publishers, Inc.: New York, **1991**; pp. 1-55.
5. Goto, H.; Osawa, E. *J. Am. Chem. Soc.* **1989**, *111*, 8950.
6. Dewar, M. J. S.; Thiel, W. *J. Am. Chem. Soc.* **1977**, *99*, 4899.
7. Funaki, Y.; Ishiguri, Y.; Kato, T.; Tanaka, S. *J. Pesticide Sci.* **1984**, *9*, 229.
8. Funaki, Y.; Ishiguri, Y.; Kato, T.; Tanaka, S. *ibid.* **1983**, *8*, 309.
9. Takano, H. *Jpn. Pestic. Inform.* **1986**, No. 49, 18.
10. Katagi, T. *J. Agric. Food Chem.* **1988**, *36*, 344.
11. Momany, F. A.; Chuman, H. *Methods in Enzym.* **1986**, *124*, 2573.
12. Yoshida, Y.; Aoyama, Y. In *In Vitro and In Vivo Evaluation of Antifungal Agents*; Iwata, K.; Vanden Bossche, H., Eds.; Elsevier Amsterdam : **1986**; pp. 123-134.
13. Poulos, T. L.; Finzel, B. C.; Gunsalus, I. C.; Wagner, G. C.; Kraut, J. *J. Biol. Chem.* **1985**, *260*, 16122.
14. Ishida, N.; Aoyama, Y.; Hatanaka, R.; Oyama, Y.; Imajo, S. ; Ishiguro, M.; Oshima, T.; Nakazato, H. ; Noguchi, T.; Maitra, U. S.; Mohan, V. P.; Sprinson, D. B.; Yoshida, Y. *Biochem. Biophys. Res. Commun.* **1988**, *155*, 317.

RECEIVED April 26, 1995